Dynamic Compressive Loading Improves Cartilage Repair in an In Vitro Model of Microfracture

Comparison of 2 Mechanical Loading Regimens on Simulated Microfracture Based on Fibrin Gel Scaffolds Encapsulating Connective Tissue Progenitor Cells

Tomoya Iseki,*† MD, Benjamin B. Rothrauff,* MD, PhD, Shinsuke Kihara,* MD, PhD, Hiroshi Sasaki,* MD, PhD, Shinichi Yoshiya,† MD, Freddie H. Fu,‡ MD, Rocky S. Tuan,*§¶ PhD, and Riccardo Gottardi,*‖¶ PhD
Investigation performed at the University of Pittsburgh, Pittsburgh, Pennsylvania, USA

Background: Microfracture of focal chondral defects often produces fibrocartilage, which inconsistently integrates with the surrounding native tissue and possesses inferior mechanical properties compared with hyaline cartilage. Mechanical loading modulates cartilage during development, but it remains unclear how loads produced in the course of postoperative rehabilitation affect the formation of the new fibrocartilaginous tissue.

Purpose: To assess the influence of different mechanical loading regimens, including dynamic compressive stress or rotational shear stress, on an in vitro model of microfracture repair based on fibrin gel scaffolds encapsulating connective tissue progenitor cells.

Study Design: Controlled laboratory study.

Methods: Cylindrical cores were made in bovine hyaline cartilage explants and filled with either (1) cartilage plug returned to original location (positive control), (2) fibrin gel (negative control), or (3) fibrin gel with encapsulated connective tissue progenitor cells (microfracture mimic). Constructs were then subjected to 1 of 3 loading regimens: (1) no loading (ie, unloaded), (2) dynamic compressive loading, or (3) rotational shear loading. On days 0, 7, 14, and 21, the integration strength between the outer chondral ring and the central insert was measured with an electroforce mechanical tester. The central core component, mimicking microfracture neotissue, was also analyzed for gene expression by real-time reverse-transcription polymerase chain reaction, glycosaminoglycan, and double-stranded DNA contents, and tissue morphology was analyzed histologically.

Results: Integration strengths between the outer chondral ring and central neotissue of the cartilage plug and fibrin + cells groups significantly increased upon exposure to compressive loading compared with day 0 controls ($P = .007$). Compressive loading upregulated expression of chondrogenesis-associated genes (SRY-related HGMG box-containing gene 9 [*SOX9*], collagen type II α1 [*COL2A1*], and increased ratio of *COL2A1* to collagen type I α1 [*COL1A1*], an indicator of more hyaline phenotype) in the neotissue of the fibrin + cells group compared with the unloaded group at day 21 (*SOX9,* $P = .0032$; *COL2A1,* $P < .0001$; *COL2A1:COL1A1,* $P = .0308$). Fibrin + cells constructs exposed to shear loading expressed higher levels of chondrogenic genes compared with the unloaded condition, but the levels were not as high as those for the compressive loading condition. Furthermore, catabolic markers (*MMP3* and *ADAMTS 5*) were significantly upregulated by shear loading ($P = .0234$ and $P < .0001$, respectively) at day 21 compared with day 0.

Conclusion: Dynamic compressive loading enhanced neotissue chondrogenesis and maturation in a simulated in vitro model of microfracture, with generation of more hyaline-like cartilage and improved integration with the surrounding tissue.

Clinical Relevance: Controlled loading after microfracture may be beneficial in promoting the formation of more hyaline-like cartilage repair tissue; however, the loading regimens applied in this in vitro model do not yet fully reproduce the complex loading patterns created during clinical rehabilitation. Further optimization of in vitro models of cartilage repair may ultimately inform rehabilitation protocols.

The American Journal of Sports Medicine
2019;47(9):2188–2199
DOI: 10.1177/0363546519855645

Keywords: microfracture; rehabilitation; mechanical loading; connective tissue progenitor cells; articular cartilage

Trauma-induced cartilage defects occur frequently in young patients and are a predisposing factor for osteoarthritis.[5] In the general population of the United States, an estimated 80,000 cartilage repair procedures are performed annually, of which the vast majority are microfractures.[34] Microfracture is a minimally invasive and inexpensive 1-step approach.[38] It consists of the targeted disruption of the subchondral bone to form a clot rich in intramedullary mesenchymal stem or marrow stromal cells (MSCs)[33,45] that fills the defect. Over time, the MSCs generate a fibrocartilaginous tissue that integrates with the surrounding hyaline cartilage. Microfracture of small lesions (<2 cm^2) yields good clinical outcomes, but efficacy is reduced with increasing lesion size.[41] Clinical improvement is observed in the majority of treated knees during the first 2 years after surgery.[23] However, at 5 years, more clinical failures are seen,[49] which are generally attributed to the inferior mechanical properties of this fibrocartilaginous repair tissue and its poor integration with the surrounding hyaline cartilage.

To enhance the quality of the newly formed tissue, various augmentation techniques using synthetic collagen matrices, scaffolds, or devices have been developed.[8,13] However, procedures aimed at augmentation of microfracture, such as autologous matrix-induced chondrogenesis, have not been thoroughly examined, and a systematic review suggested insufficient evidence to demonstrate the superiority of this technique over microfracture alone.[2,14] Therefore, there is still a pressing need to enhance chondrogenesis after microfracture so as to achieve more hyaline-like cartilage repair and improve integration with the surrounding hyaline tissue. We have focused on the mechanical environment to which early microfracture tissue may be exposed during postoperative rehabilitation, with the ultimate objective of exploring rehabilitation-driven mechanobiology to achieve better long-term repair outcomes.

In general, early passive motion and limited weightbearing are used in rehabilitation after microfracture. However, a systematic review of postoperative rehabilitation found limited evidence to support any particular regimen of passive range of motion and weightbearing exercises to improve clinical outcomes.[18] The authors concluded that additional basic science research was needed to maximize the benefits of rehabilitation protocols after cartilage repair procedures.[18] At present, it is unclear how the mechanical loads of rehabilitation regimens affect neocartilage tissue formation, as in vivo studies are limited by the inability to monitor cell responses and determine the loads that the neotissue experiences. Therefore, the purpose of this study was to use a novel in vitro model of microfracture to assess the influence of different mechanical loading regimens, including dynamic compressive loading or rotatory shear loading, on neocartilage formation.

METHODS

The in vitro model of microfracture consisted of articular cartilage plugs harvested from bovine knees, which were then centrally cored out to form a cylindrical defect space, followed by implantation of 1 of the following 3 experimental constructs: (1) cartilage core returned to the defect (positive control), (2) fibrin gel (negative control), and (3) fibrin gel containing connective tissue progenitor cells. These composite constructs were then exposed to 1 of 3 mechanical loading regimens: (1) no loading (ie, unloaded), (2) compressive loading by a MechanoActive Transduction and Evaluation (MATE) bioreactor (Mate Systems), or (3) shear loading by a rotatory cell culture system (RCCS; Synthecon Inc). At days 0, 7, 14, and 21, samples (n = 6 per group, per time point, repeated 3 times) were processed for histology (n = 6) or integration strength (n = 12). After push-out testing, half of the samples were used for gene expression profiling by quantitative reverse-transcription polymerase chain reaction (qRT-PCR) (n = 6), and the other half were used to determine biochemical composition (n = 6). The overall experimental scheme is depicted in Figure 1.

¶Address correspondence to Riccardo Gottardi, Division of Pulmonology, Department of Pediatrics, Children's Hospital of Philadelphia, Philadelphia, PA 19104, USA (email: gottardir@email.chop.edu); Rocky S. Tuan, Center for Cellular and Molecular Engineering, Department of Orthopaedic Surgery, University of Pittsburgh, Pittsburgh, PA 15219, USA. (email: rst13@pitt.edu).

*Center for Cellular and Molecular Engineering, University of Pittsburgh, Pittsburgh, Pennsylvania, USA.

†Hyogo College of Medicine, Nishinomiya, Hyōgo, Japan.

‡Department of Orthopaedic Surgery, University of Pittsburgh, Pittsburgh, Pennsylvania, USA.

§The Chinese University of Hong Kong, Hong Kong, China.

‖Fondazione Ri.MED, Palermo, Italy.

Presented at the annual meeting of the AOSSM, Boston, Massachusetts, July 2019.

The content is solely the responsibility of the authors and does not necessarily represent the official views of the National Institutes of Health.

One or more of the authors has declared the following potential conflict of interest or source of funding: R.S.T. received the MATE system free of charge as a beta tester from Apex Biomedical LLC (materials from a company that might benefit from this study). This research received funding from the Alliance for Regenerative Rehabilitation Research and Training (AR3T), which is supported by the Eunice Kennedy Shriver National Institute of Child Health and Human Development (NICHD), National Institute of Neurological Disorders and Stroke (NINDS), and National Institute of Biomedical Imaging and Bioengineering (NIBIB) of the National Institutes of Health (NIH) under award number P2CHD086843. This work is also supported, in part, by the US Department of Defense (W81XWH-14-2-0003 to R.S.T), by the EU Horizon 2020 - Research and Innovation Action SC1-PM 17 - 2017 +Project OACTIVE (under Grant Agreement No. 777159 to R.G.), and by Fondazione Ri.MED (grant to R.G.). AOSSM checks author disclosures against the Open Payments Database (OPD). AOSSM has not conducted an independent investigation on the OPD and disclaims any liability or responsibility relating thereto.

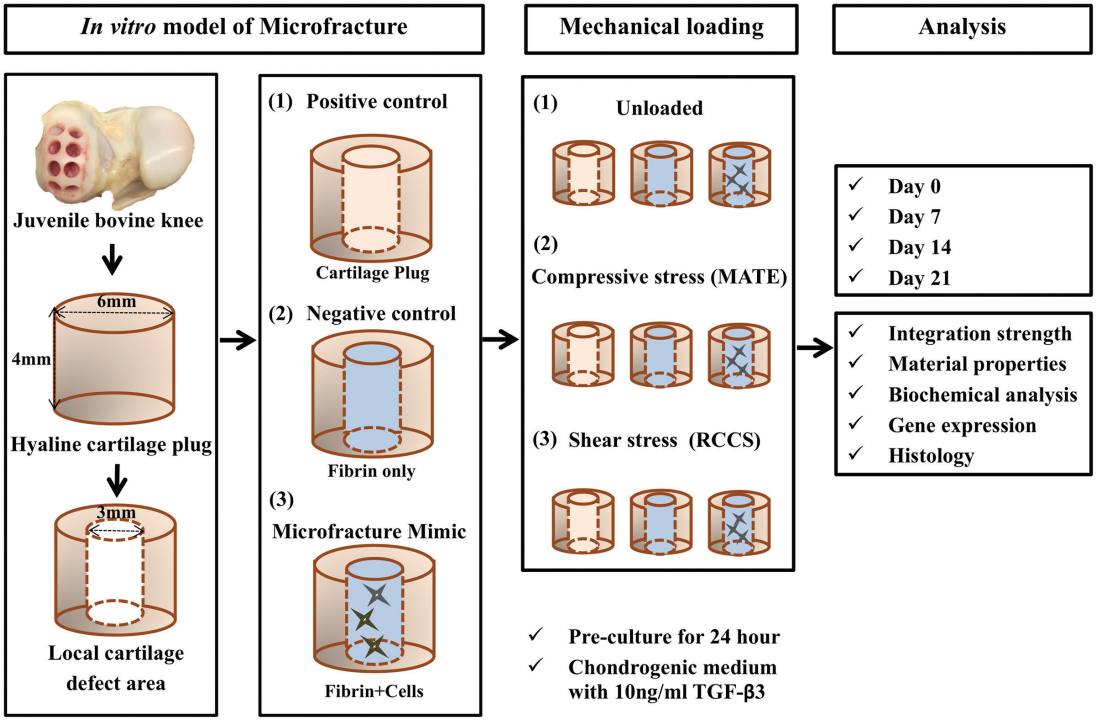

Figure 1. Schematic of experimental design. The in vitro model of microfracture consisted of articular cartilage plugs harvested from bovine knees, which were then centrally cored out to form a cylindrical defect space, followed by implantation of 1 of the following 3 experimental constructs: (1) positive control (inner plug returned to the defect), (2) negative control (fibrin only), and (3) microfracture mimic (fibrin + cells). These composite constructs were then exposed to 1 of 3 mechanical loading regimens: (1) unloaded, (2) compressive loading (MechanoActive Transduction and Evaluation bioreactor; MATE), and (3) shear loading (rotatory cell culture system; RCCS). At the end of the indicated experimental periods, some samples (n = 2 per group, per time point) were processed for histological analysis, and the remaining samples (n = 4) were evaluated by push-out test. After testing, half of the samples were processed for gene expression profiling by quantitative reverse-transcription polymerase chain reaction (n = 2) and for biochemical analysis (n = 2). TGF-β3, transforming growth factor β3.

Connective Tissue Progenitor Cell Isolation

Bone marrow aspirates were harvested from the subchondral trabecular bone of juvenile bovine hindlimbs (3-6 months old, within 24 hours of slaughter) and culture expanded as previously described.[19,21,31] In brief, bone marrow was flushed from the trabecular bone of the femoral neck by use of an 18-gauge needle and was mixed with expansion medium, consisting of the following: Dulbecco's modified Eagle's medium (DMEM) supplemented with 10% fetal bovine serum and 1% antibiotics-antimycotic (ampicillin, 100 U/mL; streptomycin, 100 μg/mL; amphotericin B, 250 ng/mL) supplemented with 300 U/mL heparin. The suspension was vortexed to remove any remaining fat and bone fragments from the marrow, passed through a 100-μm cell strainer, and centrifuged at 300*g* for 5 minutes to collect cell pellets. Cells were resuspended in the expansion medium supplemented with 1.5 ng/mL recombinant human fibroblast growth factor 2 (RayBiotech) and plated onto T-150 flasks, with medium changes every 3 to 4 days. Once 70% to 80% confluence was reached, cells were passaged. All experiments were performed with passage 3 bovine connective tissue progenitor cells.

Preparation of Fibrin Gel

Fibrin gels were prepared by use of the Tisseel fibrin glue kit (Baxter) and modified based on previous reports.[3,11,27] To make cell-seeded fibrin gels, fibrinogen containing cells at 10×10^6 cells/mL was dissolved in dilution buffer (Sealer protein solution; 3000 KIE/mL aprotinin) at a concentration of 100 mg/mL, mixed with thrombin at a concentration of 5 U/mL in 40 mM $CaCl_2$, and pipetted (30 μL) into the center of each chondral ring (prepared as described below). The fibrin filler, with or without cells, was incubated for 30 minutes at 37°C to allow formation and stabilization of the hydrogel.

Microfracture Model Preparation

Cartilage plugs (6-mm diameter, 4-mm thickness) were harvested via biopsy punch from the femoral condyles of juvenile bovine knees, and cylindrical cores (3-mm diameter) were separated from the plug center to mimic a local defect area. The defects were filled with the same inner cartilage core returned to its original location (positive control), fibrin gel only (cell-free, negative control), or fibrin gel

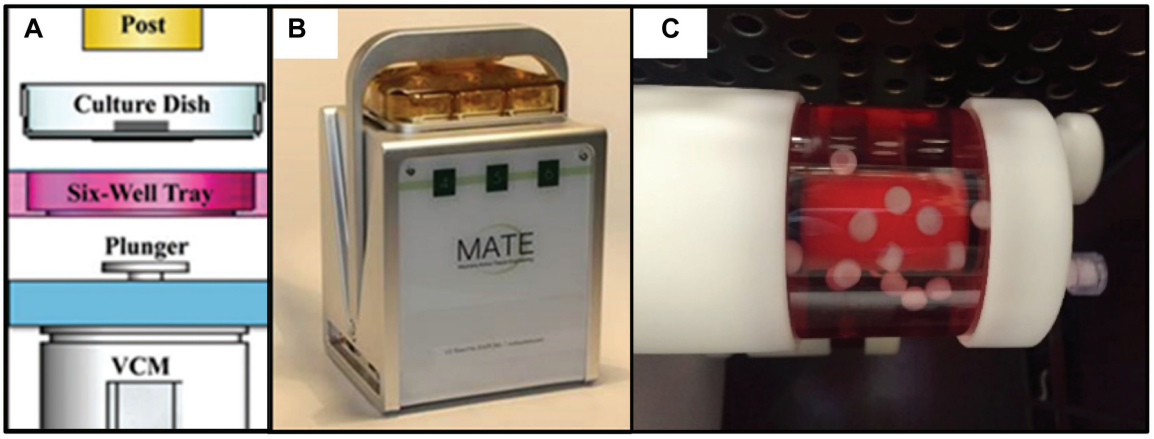

Figure 2. Mechanical loading of cartilage microfracture models in culture. (A) Schematic image of MechanoActive Transduction and Evaluation (MATE) bioreactor. The electromagnetic coil motor (VCM) raises the plunger and culture dish, thereby compressing specimens onto impermeable posts. Adapted with permission from Lujan TJ, Wirtz KM, Bahney CS, Madey SM, Johnstone B, Bottlang M. A novel bioreactor for the dynamic stimulation and mechanical evaluation of multiple tissue-engineered constructs. *Tissue Eng Part C Methods.* 2011;17(3):367-374.[28] (B) The compact-sized MATE readily fits into standard incubators. (C) Rotatory cell culture system in the incubator.

containing 10×10^6 cells/mL (n = 6 per group, per time point, repeated 3 times for different donors). The composite constructs were cultured in chondrogenic medium, which contained the following: DMEM with 1% L-alanyl-L-glutamine, 55 μM sodium pyruvate, 1× antibiotic-antimycotic, 1% insulin-transferrin-selenium (Invitrogen), 10 ng/mL transforming growth factor β3 (TGF-β3; PeproTech), 100 nM dexamethasone, 50 μM L-ascorbic acid 2-phosphate, and 23 μM L-proline. After 24 hours of culture, the constructs were subjected to 1 of 3 loading regimens.

Mechanical Loading

Dynamic compressive loading was provided using the MATE bioreactor system (Figure 2), which allows the application of cyclic compression to tissues with controlled force and displacement within an incubator (37°C, 5% CO_2, and 85% humidity).[28] To mimic a cadence as might be performed during a post-microfracture progressive weight-bearing rehabilitation protocol, the MATE system was operated at 1.5 Hz for 2 minutes followed by a 2-minute pause between each sequence with a 9-N load force, for 1 hour a day, over 21 consecutive days. Continuous shear loading was provided by a rotatory cell culture system (RCCS TM-4; Synthecon Inc). The rotation speed applied was between 22 and 25 rpm to maintain a stable free-falling position[24] with the cartilage cylindrical axis mostly perpendicular to the fluid flow. All samples were maintained in chondrogenic medium. The volume of medium per construct was equivalent among all loading conditions, and medium change occurred at the same frequency for all samples. After 21 days of loading or static culture (ie, unloaded), samples were collected for analysis.

Testing of Integration Strength

After culturing for the designated period of time, tissue integration for each group was assessed by push-out testing with a mechanical tester (ElectroForce 3200; Bose). A 2 mm–diameter, flat-ended cylindrical indenter was aligned above a sample support plate with a 4 mm–diameter hole as described by Coluccino et al[9] (Figure 3). In brief, the cartilage model was placed on the support plate, and the indenter was pressed through the defect site at a rate of 0.08 mm/s. Integration strength was calculated as the ratio of the maximum force registered over the external surface between the cartilage outer rim and the cartilage plug, fibrin, or fibrin + cells, as described above.

Histology and Immunohistochemistry

Constructs were fixed in 4% paraformaldehyde overnight at 4°C; equilibrated in 10% (wt/vol) sucrose, 20% sucrose, and 30% sucrose for 1 hour each; embedded in Tissue-Tek Optimal Cutting Temperature compound (Sakura Finetek USA); and cryosectioned at 10-μm thickness. The sections were stained with Safranin O/Fast Green and Toluidine Blue (Polysciences) for histological examination of cell morphology, extracellular matrix deposition, and integration between the central core and outer chondral ring. For immunohistochemistry, deparaffinized and rehydrated sections were incubated with primary antibodies against bovine proteoglycan 4 (PRG4; Abcam) at 4°C overnight, followed by incubation with appropriate secondary antibodies. Immunostaining was carried out with the Vectastain ABC kit and NovaRED peroxidase substrate kit (Vector Laboratories).

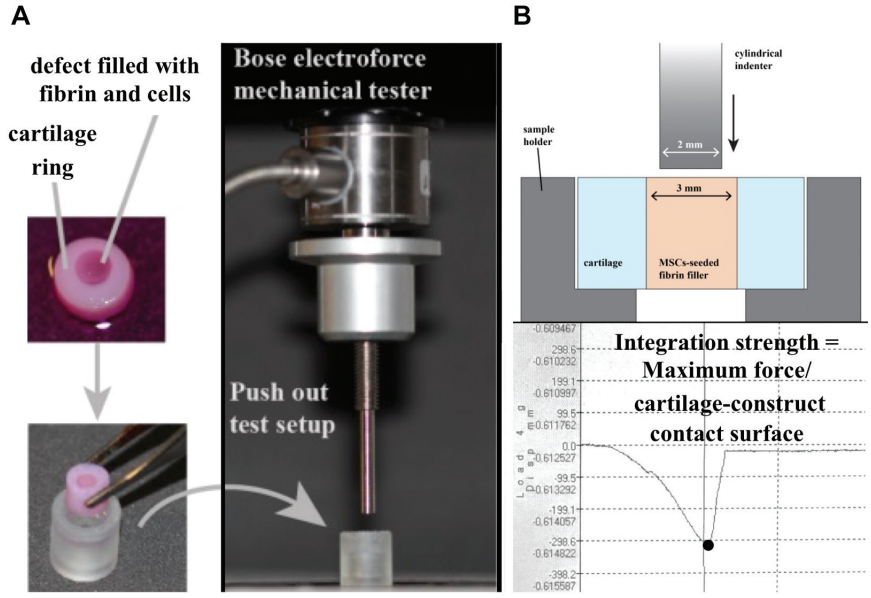

Figure 3. Measurement of integration strength between central core and outer hyaline cartilage ring. (A) Depiction of cartilage microfracture model and photograph of push-out test setup. (B) Cross-sectional schematics of the push-out test setup. Integration strength was calculated as the ratio of the maximum force registered over the contact surface between the outer ring and inner core.

Biochemical Composition

Cartilage extracellular matrix (ECM) deposition in fibrin inserts was quantified by measuring sulfated glycosaminoglycan (sGAG) production normalized by double-stranded DNA (dsDNA) content. Constructs were homogenized and then digested for 18 hours in 500 μL/construct papain solution (125 mg/mL papain, 50 mM sodium phosphate buffer, 2 mM N-acetyl cysteine [Sigma], pH 6.5). An aliquot of the digest was assayed for sGAG content through use of the Blyscan kit (Accurate Chemical & Scientific Corp) according to the manufacturer's instructions. Another aliquot of the digest was assayed for dsDNA content by use of the QuantiT PicoGreen dsDNA Assay Kit (Invitrogen).

Real-Time PCR Analysis of Gene Expression

As described above, samples were separated into the core and chondral outer ring by use of the Electroforce mechanical tester at days 0, 7, 14, and 21 and were then frozen at –80°C for analysis at a later date. Total cellular RNA was isolated with the RNeasy kit (Qiagen), and first-strand cDNA was synthesized with the SuperScript III First-Strand cDNA synthesis kit (Invitrogen). Real-time RT-PCR was performed by use of SYBR green Supermix in a Step One Plus real-time PCR system (Applied Biosystems, Life Technologies). The target genes and sequences of primers are shown in Table 1. RT-PCR was used to determine the relative expression of aggrecan (*ACAN*), collagen type I α1 (*COL1A1*), collagen type II α1 (*COL2A1*), SRY-related HGMG box containing gene 9 (*SOX9*), matrix metalloproteinase 3 (*MMP3*), a disintegrin and metalloproteinase with thrombospondin motifs 5 (*ADAMTS5*), and *PRG4*, with *18S* rRNA as the housekeeping reference gene. The relative expression level of each gene in a given group was normalized to the expression level on day 0 using the ΔΔCt method.

Elastic Moduli of Constructs Under Compressive Loading

For constructs in the compressive loading condition, daily mechanical tests were automatically performed to measure material properties during 21 days of culture under standard incubation conditions (37°C, 5% CO_2). Before each mechanical test, the specimen thickness was measured automatically by the MATE system after a preload of 0.5 N was applied. Elastic moduli were automatically calculated, as described previously, at a load rate of 10 N/s.[28]

Statistical Analysis

All data were expressed as mean ± SD, and statistical analysis was performed using either 2-way independent analysis of variance or 2-way independent multivariate analysis of variance, followed by Tukey HSD post hoc testing. A threshold of $P < .05$ was adopted to determine statistical significance.

RESULTS

Integration Between Articular Cartilage and Implanted Core

All experimental groups showed a general tendency of increasing integration strength between the outer hyaline

TABLE 1
Real-Time Polymerase Chain Reaction Primers and Predicted Product Sizes[a]

Gene	Sequence (5′-3′)	Size, base pairs
SOX9	Sense: AATCTCCTGGACCCCTTCATG	60
	Antisense: GGCGGACAGGCCCTTCT	
COL2A1	Sense: AAGAAGGCTCTGCTCATCCAGG	124
	Antisense: TAGTCTTGCCCCACTTACCGGT	
ACAN	Sense: CCTGAACGACAAGACCATCGA	101
	Antisense: TGGCAAAGAAGTTGTCAGGCT	
COL1A1	Sense: AAGAACCCAGCTCGCACATG	82
	Antisense: GGTTAGGGTCAATCCAGTAGTAACCA	
MMP3	Sense: TGGTCCAGGAGATGAAGACC	109
	Antisense: TGGCATCAAGGGATAAGGAA	
ADAMTS5	Sense: CTCCCATGACGATTCCAA	85
	Antisense: AATGCTGGTGAGGATGGAAG	
PRG4	Sense: AGAAAACCCGATGGCTATGA	106
	Antisense: TCGCCCATCAGTCTAAGGAC	
18S rRNA	Sense: TCGAGGCCCTGTAATTGGAA	104
	Antisense: GCTATTGGAGCTGGAATTACCG	

[a]*ACAN*, aggrecan; *ADAMTS*, a disintegrin and metalloproteinase with thrombospondin motifs; *COL1A1*, collagen type I α1; *COL2A1*, collagen type II α1; *MMP*, matrix metalloproteinase; *PRG*, proteoglycan; *SOX9*, SRY-related HGMG box containing gene 9; *18S rRNA*, 18S ribosomal RNA.

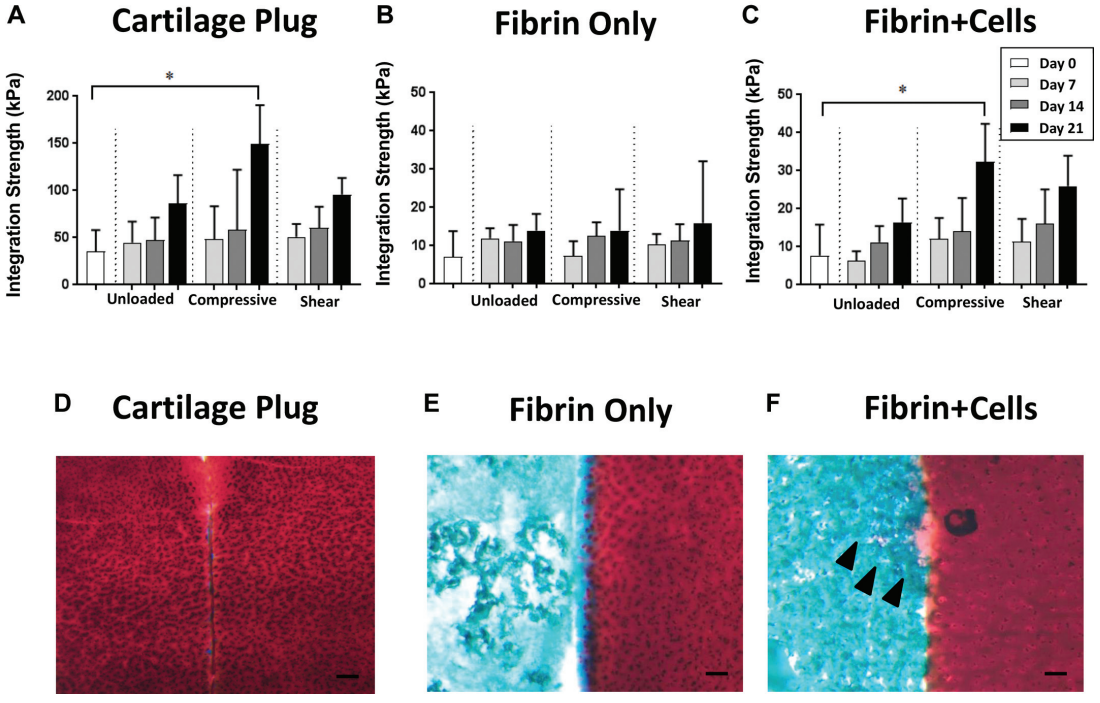

Figure 4. Integration between outer cartilage ring and central insert. (A-C) Integration strength between outer hyaline chondral ring and central insert of (A) cartilage plug, (B) fibrin only, and (C) fibrin + cells, compared with day 0 (control), $P < .05$. (D-F) Safranin O/Fast Green histological staining of the interface between outer hyaline chondral ring and central insert: (D) cartilage plug, (E) fibrin only, and (F) fibrin + cells at day 14 in the compressive loading condition. Arrowheads indicate pericellular deposition of proteoglycan. Bar, 100 μm; n = 12, combined from 3 independent trials.

cartilage ring and the central core as a function of culture time. Although the fibrin gel group exhibited no differences among the 3 loading conditions (Figure 4B), in the cartilage plug and the fibrin + cells groups, the samples subjected to compressive loading showed significantly higher integration strength at day 21 compared with day 0 controls ($P = .001$ and $P = .007$, respectively); in comparison, in the unloaded and shear loading conditions, no significant differences were seen with time (Figure 4, A and C).

Histological analysis showed that the outer cartilage rings harvested from bovine cartilage continued to exhibit chondrocytes embedded in a proteoglycan-rich extracellular matrix, evidenced by intense Safranin O (red) staining (Figure 4, D-F). Upon examination of the border between the outer cartilage ring and the central insert, the cartilage plug that was returned to its original location showed red Safranin O staining in both cartilage elements, but there was a small gap between the inner and outer hyaline cartilage components (Figure 4D). In comparison, in the fibrin gel group, voids were seen in the hydrogel itself, and the hydrogel was only intermittently in contact with the cartilage ring (Figure 4E). Conversely, for the fibrin + cells group, chondrocyte-like cells were seen surrounded by a matrix with more robust Safranin O staining, and no obvious gap was seen at the border of the outer and inner components (Figure 4F).

Histology, Immunohistochemistry, and Biochemical Composition of Neocartilage Repair Tissue Under Different Loading Conditions

Histological evaluation of matrix deposition in the fibrin + cells group showed different effects of the 3 loading conditions (Figure 5A). At culture day 7, all 3 conditions—unloaded, compressive loading, and shear loading—appeared similar to day 0 controls, with the visual absence of proteoglycan (red) staining. However, by day 21, both the unloaded and compressively loaded groups stained more strongly for proteoglycan content than the shear loaded constructs. At the same time, there appeared to be greater pore sizes in the unloaded constructs compared with the loaded constructs. Conversely, no loading condition preferentially upregulated the synthesis of PRG4 (Appendix Figure A1A, available in the online version of this article).

Analysis of biochemical composition demonstrated a similar pattern as histological testing (Figure 5B). By day 21, normalized glycosaminoglycan production (GAG/DNA) was significantly higher in the unloaded (P = .019) and compressively loaded (P = .003) constructs compared with day 0 controls. Although the unloaded and compressively loaded constructs possessed greater relative GAG production at earlier time points (ie, days 7 and 14) compared with day 0, these differences did not reach statistical significance. Interestingly, normalized GAG content did not increase over time in the shear loading condition. Acellular fibrin constructs, regardless of loading condition, contained undetectable GAG content and low dsDNA content, suggesting minimal migration of native chondrocytes from the cartilage ring into the fibrin insert (Appendix Figure A2, available online).

Gene Expression

We next examined how the emergence of a chondrogenic phenotype in the fibrin + cells microfracture model was affected by culturing under different mechanical activations. Upregulation of chondrogenic gene markers,

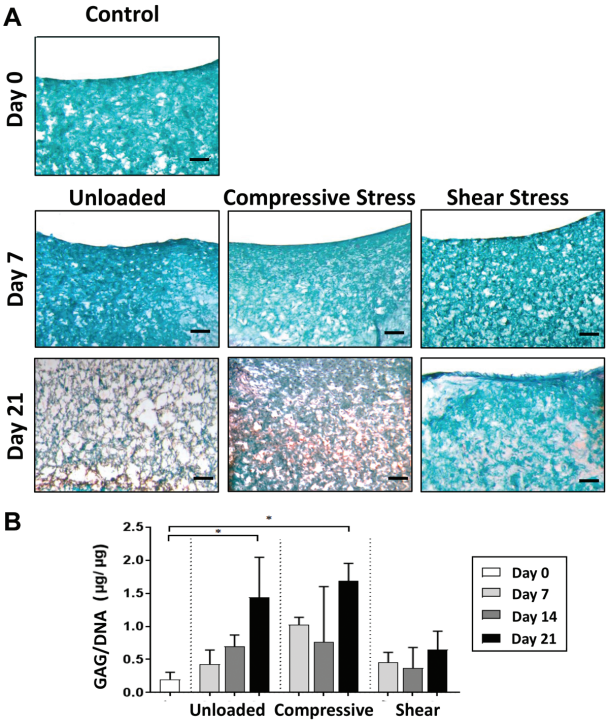

Figure 5. Safranin-O/Fast Green staining of fibrin with cells. (A) Day 0 controls and days 7 and 21 by loading condition; scale bar = 200 μm. Glycosaminoglycan (GAG) stained red, and fibrin stained blue/green, showing higher GAG content in unloaded and compressive loading conditions at day 21. (B) Normalized glycosaminoglycan content (GAG/DNA) as a function of culture time by loading condition. *Significantly higher than day 0 controls ($P < .05$).

including *SOX9, COL2A1*, and *ACAN*, was not significantly different among the 3 loading conditions until day 14 (Figure 6, A-C). However, at day 21, expression of the chondrogenesis-associated genes in the compressive loading group was significantly higher compared with day 0 controls (*SOX9,* P = .0034; *COL2A1,* $P < .0001$; *ACAN,* P = .0141) and compared with the unloaded constructs at the same time point (*SOX9,* P = .0032; *COL2A1,* $P <$ .0001; *ACAN,* P = .0151) (Figure 6, A-C). Furthermore, the *COL2:COL1* ratio, an indicator of a more hyaline phenotype compared with a fibrochondrogenic phenotype of the neotissue, was most upregulated with compressive loading compared with the unloaded condition at day 21 (P = .0308). In contrast, expression of chondrogenesis-associated genes in the shear loading condition was significantly higher than the unloaded group at day 21 only for *SOX9* (P = .0208), and the difference was much less pronounced than for the compressive loading group. Furthermore, the catabolic markers, *MMP3* and *ADAMTS5*, were significantly upregulated with shear loading (P = .0234, $P < .0001$, respectively) at day 21. Consistent with the results from immunohistochemistry, no loading condition significantly upregulated *PRG4* expression (Appendix Figure A1B, available online)

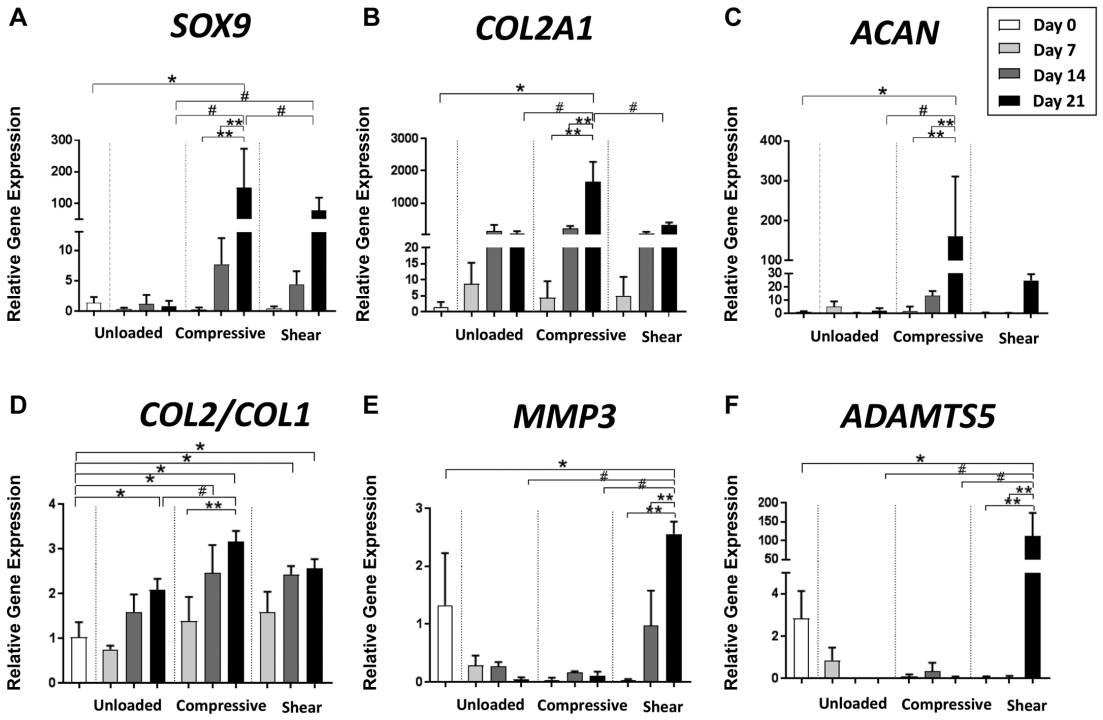

Figure 6. Gene expression of fibrin + cells group cultured under 3 mechanical loading conditions. Gene expression was analyzed by quantitative reverse-transcription polymerase chain reaction for (A) *SOX9*, (B) *COL2A1*, (C) *ACAN*, (D) *COL2:COL1* (ratio of collagen type II to collagen type I), (E) *MMP3*, and (F) *ADAMTS5*. All expression levels are expressed relative to day 0 controls. *Comparison with day 0 controls ($P < .05$). **Comparison with other time points within the same activation group ($P < .05$). #Comparison between activation groups at the same time point ($P < .05$). *ACAN*, aggrecan; *ADAMTS*, a disintegrin and metalloproteinase with thrombospondin motifs; *COL1A1*, collagen type I α1; *MMP*, matrix metalloproteinase; *SOX9*, SRY-related HGMG box containing gene 9.

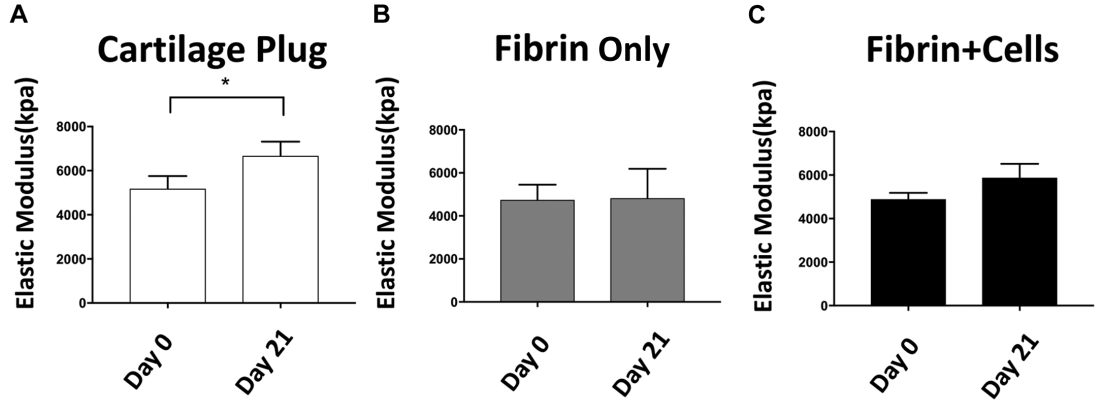

Figure 7. Elastic moduli of composite constructs at days 0 and 21. (A) cartilage plug, (B) fibrin only, and (C) fibrin + cells. *$P < .05$.

Modulus of Cartilage Exposed to Compressive Loading for 21 Days

As determined automatically by the MATE system before the commencement of each compressive loading treatment each day, the elastic modulus of the cartilage plug group was significantly increased by day 21, compared with day 0 (Figure 7A). Although a similar trend was seen in the fibrin + cells group, the increase did not reach statistical significance (Figure 7C). The moduli of the fibrin-only constructs were equivalent on day 0 and day 21 (Figure 7B). No statistically significant differences were found at earlier time points (ie, days 7 and 14) for any group (data not shown).

DISCUSSION

In this study, we developed an in vitro model of the microfracture procedure for articular cartilage repair by using a composite explant consisting of a native articular cartilage ring filled with fibrin hydrogel containing connective tissue progenitor cells. A key finding of the present work is that exposure to dynamic compressive loading in the in vitro microfracture mimic both enhances the hyaline cartilage phenotype of the new repair tissue and improves the strength of integration with the surrounding hyaline cartilage.

The most common rehabilitation protocol after microfracture prescribes no weightbearing for 2 weeks, followed by up to 8 weeks of passive range of motion (ROM) exercise produced by a continuous passive motion (CPM) device, primarily aimed at avoiding joint stiffening.[35,45] Some in vitro evidence shows that ROM could stimulate proteoglycan metabolism[22,37,43] and that postoperative ROM could stimulate the cellular response in an implanted graft, resulting in neomatrix production.[43,51] Exploring this possibility, Nugent-Derfus et al[37] reported that CPM of explanted bovine knee joints induced PRG4 expression after 24 hours of continuous stimulation. However, this report was limited in terms of clinical relevance due to the short experiment duration (ie, stimulation for only 24 hours) and did not allow extrapolation to the potential biological effect of long-term application of CPM to human joints. In comparison, our 21-day study did not highlight any significant upregulation of PRG4 by any of the applied loading regimens, which may represent a limitation of our in vitro culture system. As for longer term effects of CPM, a clinical study by Marder et al[29] found no difference in clinical outcomes at a mean of 4.2 years after microfracture between patients who were nonweightbearing with CPM versus patients allowed to bear weight as tolerated without CPM.

In general, few studies have sought to mimic the joint loading conditions to evaluate the efficacy of rehabilitation regimens after microfracture. To this end, we have drawn from the field of tissue engineering, where the use of bioreactors to deliver controlled mechanical loads and of scaffolds to host stem cells is well-established.[4,17,21] However, unlike authors who used standard cartilage tissue engineering, we did not focus on generating in vitro biological substitutes for defect repair but rather focused on modelling the native MSC-rich clot that forms within the defect after microfracture. In the literature, a number of different culturing and loading conditions are described to promote engineered cartilage maturation,[13] sometimes reporting opposing results that can depend on the specific combination of bioreactor, scaffolds, growth factor supplementation, and loading used. For instance, Thorpe et al[48] reported that compressive loading inhibited chondrogenesis of MSCs, whereas Mauck et al[31] demonstrated enhanced chondrogenesis after compressive mechanical activation. Notably, Thorpe et al[48] included TGF-β as a medium supplement whereas Mauck et al[31] did not, suggesting a nuanced relationship between biochemical and mechanical cues. In reviewing the chondrogenic response of MSCs to mechanical cues in the absence of exogenous growth factors, Fahy et al[12] found consistent upregulation of TGF-β expression in mechanically activated MSCs, presumably serving as an autocrine/paracrine factor to enhance chondrogenesis. As the current study found enhanced chondrogenesis due to compressive loading in the presence of exogenous TGF-β, it is possible that the relative effect of compressive loading in the absence of exogenous growth factors would have been even more dramatic, although these experiments were not performed. Furthermore, Schätti et al[44] explored how combining shear and compressive loading led to mechanically induced chondrogenesis without exogenous growth factors. In a follow-up study, Gardner et al[15] confirmed that the combination of shear and compressive loading transformed the endogenously secreted TGF-β from its inactive to its active form, resulting in enhanced chondrogenesis.[16] In our work, TGF-β was already present in the medium, and shear and compressive loadings were not combined. These in vitro conditions allowed us to explore the specific effect of each loading regimen on cell differentiation, independently from the contribution of mechanically mediated TGF-β activation. Admittedly, this is different from in vivo gait modeling, where cartilage experiences forces in multiple directions. Nonetheless, in the present study we have paid particular attention to clinical relevance after microfracture and have therefore selected loading conditions to approximate the more limited motion in the articular joint environment during rehabilitation. Specifically, we applied cyclic compression in sequences timed to those of partial weightbearing exercises using the MATE system with force control.[28] To model the shear stress caused by the flow of synovial fluid on articular cartilage during unloaded ROM,[6,44] we used RCCS, consisting of a rotating wall vessel filled with medium that generates low shear stress[39,42] and supports perfusion of nutrients.[32,39,52]

The RCCS has been frequently used to successfully engineer cartilage starting from stem cells. For instance, Yu et al[53] used adipose-derived MSCs to create cartilaginous constructs with marked *COL2A1* upregulation, and Marsano et al[30] exploited the hydrodynamic forces within the RCCS to generate cartilaginous constructs with an anisotropic structure mimicking native tissue. To the best of our knowledge, however, our work is the first instance of using the RCCS with a cartilage repair model. In our microfracture mimic in the RCCS, we observed an increase in chondrogenic gene expression compared with unloading, highlighting the anabolic and prochondrogenic response induced by fluid flow in the bioreactor. However, increased gene expression was not accompanied by an increase in GAG production compared with control. Moreover, the COL2:COL1 ratio did not change significantly from unloading, suggesting that shear forces alone do not shift the differentiation process of the repair tissue toward a more chondrogenic phenotype. Notably, in the RCCS, a marked increase in *MMP3* and *ADAMTS5* gene expression was also observed, which is associated with a catabolic response or with attempts at remodeling by the differentiating cells. Finally, we found a mild trend toward higher integration strength with the surrounding hyaline cartilage but no significant increase when compared with day 0 controls. This

finding indicates that even if remodeling was taking place, at 21 days the overall outcome of repair was limited and the overall expression of chondrogenic genes in the RCCS did not match that obtained by compressive loading.

In terms of compressive loading parameters, most studies have used a frequency of 1 Hz and reported chondrogenic differentiation of scaffold-encapsulated MSCs.[22,36,37,51] However, the walking cadence of a healthy human is approximately 1.8 Hz,[10,50] and an intermittent gait is expected during postsurgical rehabilitation. Therefore, in this study, we set a frequency of 1.5 Hz for 2 minutes followed by 2 minutes for rest, repeated for 1 hour. In a study involving intermittent loading reported by Steinmetz and Bryant,[46] the loading regimen was set at 0.5 hours of stimulation followed by 1.5 hours of rest; under dynamic loading, the expression of cartilage-related markers (*SOX9*, *COL2A1* and *ACAN*) was downregulated, which appears to be in contrast to our findings. However, Steinmetz and Bryant used long intermittent intervals and long durations of loading (16 hours per day). Other studies have recommended a loading duration of 1 to 4 hours per day, which was found to be sufficient to induce MSC chondrogenesis, whereas longer loading durations (eg, 12 and 24 hours per day) may cause cell apoptosis.[7,40] In fact, Steinmetz and Bryant reported that nonchondrogenic genes were also downregulated, suggesting a general metabolic effect. Furthermore, the compressive loading regimen was performed in displacement control, which results in a much smaller stimulation because of the rapid cartilage relaxation[47] and does not simulate well the human gait, which is characterized by the applied load dependent on body weight (load control).

In additional studies involving longer experimental time frames, Huang et al[20] reported that the expression of chondrogenic markers, including collagen type II and aggrecan, increased after 1 and 2 weeks of loading for 4 hours per day but returned to baseline levels after an additional week of loading. Thorpe et al[48] reported that GAG content was significantly higher in unloaded constructs compared with compressively loaded constructs at 42 days. When we consider these reported findings, the short intermittent interval as applied in our study appears to be more effective in inducing chondrogenic differentiation, although a direct comparison of different loading durations was not performed. Another major difference between our study and other tissue-engineering approaches where mechanical loading is applied to cell-seeded scaffolds is that the constructs are biphasic structures where the developing "repair cartilage" is surrounded by a hyaline cartilage ring, thus mimicking a local cartilage defect area (eg, in the knee joint) repaired by microfracture. Although this experimental approach more closely models the in vivo microenvironment of cartilage repair, assays were not universally performed for both the neotissue implant and the surrounding cartilage ring (eg, for measuring elastic modulus), limiting our ability to probe how the loading protocols affected the individual elements of the in vitro microfracture model.

Our findings support the concept that chondrogenesis of connective tissue progenitor cells can be modulated by mechanical activation. In particular, we observed that mechanical regimens of dynamic compression upregulated chondrogenic gene markers, including a higher *COL2:COL1* ratio at day 21, suggesting a less fibrous and more hyaline phenotype of the repair tissue. Corresponding to higher aggrecan gene expression, compressive loading also produced neotissue with higher GAG/DNA at day 21 compared with constructs subjected to rotatory shear stress. Integration strength with the surrounding hyaline cartilage was also higher for the compressive loading condition than the shear loading condition. Taken together, these results suggest that compressive loading after microfracture may be beneficial in promoting the formation of more hyaline-like cartilage repair tissue as well as favoring better integration between the newly formed tissue and the surrounding native cartilage. Nevertheless, the individual loading modalities used herein do not fully reproduce the complex patterns of stresses created during joint loading, as experienced during postoperative rehabilitation. Specific recommendations regarding postoperative rehabilitation cannot be made based on these early findings, which can instead inform the design of more comprehensive studies, both in vitro and in vivo, to explore the specific role of rehabilitation protocols on cartilage repair.

Our study had several limitations. First, the in vitro microfracture model was composed of a cartilage ring that lacked subchondral bone, which is known to play an integral role in maintaining osteochondral health[1] and mediating outcomes of microfracture. Although dynamic compression was applied to the cartilage construct positioned on a stiff well bottom, shear stress applied in the RCCS was experienced on both sides of the cartilage construct, in contrast to the in vivo joint in which shear forces are principally applied to the superficial cartilage. Second, we did not test the combination of shear loading and compressive loading; namely, in each bioreactor, only 1 mode of mechanical activation was studied. This allowed us to explore the effects of orthogonal modes of mechanical loading but did not capture the effect of their combination,[44] including, for instance, transformation of latent TGF-β to its active, prochondrogenic form as reported by Gardner et al.[15] Third, we did not measure GAG content in the medium. Related studies have suggested that the majority of cell-secreted GAG is released into the medium[25] rather than bound to a surrounding fibrin matrix. The low normalized GAG content seen in the shear loading condition might be attributable, in part, to preferential loss of GAG into the medium. Fourth, the fibrin + cells group does not reconstitute the complex combination of proteins and heterogeneous cell populations found in the microfracture clot, nor do culture media capture the full complexity of synovial fluid. In future studies, we plan to examine the influence of sequential exposure to different mechanical activation modalities with respect to both chondrogenic differentiation and tissue integration, to mimic different sequences of rehabilitation regimens. Additionally, we may apply simultaneous compression and shear, use blood products (eg, clots, platelet-rich fibrin), and supplement the medium with synovial fluid components, to more fully model the joint microenvironment.

CONCLUSION

Using an in vitro model of microfracture repair of a focal cartilage defect, we found that compressive loading not only positively affected the generation of a more hyaline cartilage phenotype but also promoted higher integration strength between the native and nascent repair cartilage. In comparison, exposure to shear stress did not yield similar improvements and, additionally, resulted in significantly upregulated expression of catabolic markers by culture day 21. These findings suggest that compressive loading after microfracture may be beneficial in promoting the formation of more hyaline-like cartilage repair tissue; however, corroboration by clinical studies is needed.

ACKNOWLEDGMENT

The authors thank Apex Biomedical LLC for the use of the MATE system free of charge.

REFERENCES

1. Alexander PG, Gottardi R, Lin H, Lozito TP, Tuan RS. Three-dimensional osteogenic and chondrogenic systems to model osteochondral physiology and degenerative joint diseases. *Exp Biol Med (Maywood)*. 2014;239(9):1080-1095.
2. Anders S, Volz M, Frick H, Gellissen J. A randomized, controlled trial comparing autologous matrix-induced chondrogenesis (AMIC(R)) to microfracture: analysis of 1- and 2-year follow-up data of 2 centers. *Open Orthop J*. 2013;7:133-143.
3. Bensaid W, Triffitt JT, Blanchat C, Oudina K, Sedel L, Petite H. A biodegradable fibrin scaffold for mesenchymal stem cell transplantation. *Biomaterials*. 2003;24(14):2497-2502.
4. Bian L, Zhai DY, Zhang EC, Mauck RL, Burdick JA. Dynamic compressive loading enhances cartilage matrix synthesis and distribution and suppresses hypertrophy in hMSC-laden hyaluronic acid hydrogels. *Tissue Eng Part A*. 2012;18(7-8):715-724.
5. Buckwalter JA, Saltzman C, Brown T. The impact of osteoarthritis: implications for research. *Clin Orthop Relat Res*. 2004;427(suppl):S6-S15.
6. Chen C, Tambe DT, Deng L, Yang L. Biomechanical properties and mechanobiology of the articular chondrocyte. *Am J Physiol Cell Physiol*. 2013;305(12):C1202-C1208.
7. Choi JR, Yong KW, Choi JY. Effects of mechanical loading on human mesenchymal stem cells for cartilage tissue engineering. *J Cell Physiol*. 2018;233(3):1913-1928.
8. Chu CR, Fortier LA, Williams A, et al. Minimally manipulated bone marrow concentrate compared with microfracture treatment of full-thickness chondral defects: a one-year study in an equine model. *J Bone Joint Surg Am*. 2018;100(2):138-146.
9. Coluccino L, Gottardi R, Ayadi F, Athanassiou A, Tuan RS, Ceseracciu L. Porous Poly(vinyl alcohol)-Based Hydrogel for Knee Meniscus Functional Repair. *ACS Biomater Sci Eng*. 2018;4(5):1518-1527.
10. Elder BD, Athanasiou KA. Hydrostatic pressure in articular cartilage tissue engineering: from chondrocytes to tissue regeneration. *Tissue Eng Part B Rev*. 2009;15(1):43-53.
11. Eyrich D, Brandl F, Appel B, et al. Long-term stable fibrin gels for cartilage engineering. *Biomaterials*. 2007;28(1):55-65.
12. Fahy N, Alini M, Stoddart MJ. Mechanical stimulation of mesenchymal stem cells: implications for cartilage tissue engineering. *J Orthop Res*. 2018;36(1):52-63.
13. Filardo G, Kon E, Roffi A, Di Martino A, Marcacci M. Scaffold-based repair for cartilage healing: a systematic review and technical note. *Arthroscopy*. 2013;29(1):174-186.
14. Gao L, Orth P, Cucchiarini M, Madry H. Autologous matrix-induced chondrogenesis: a systematic review of the clinical evidence. *Am J Sports Med*. 2019;47(1):222-231.
15. Gardner OFW, Fahy N, Alini M, Stoddart MJ. Joint mimicking mechanical load activates TGFbeta1 in fibrin-poly(ester-urethane) scaffolds seeded with mesenchymal stem cells. *J Tissue Eng Regen Med*. 2017;11(9):2663-2666.
16. Gottardi R, Stoddart MJ. Regenerative rehabilitation of the musculoskeletal system. *J Am Acad Orthop Surg*. 2018;26(15):e321-e323.
17. Guo T, Yu L, Lim CG, et al. Effect of dynamic culture and periodic compression on human mesenchymal stem cell proliferation and chondrogenesis. *Ann Biomed Eng*. 2016;44(7):2103-2113.
18. Howard JS, Mattacola CG, Romine SE, Lattermann C. Continuous passive motion, early weight bearing, and active motion following knee articular cartilage repair: evidence for clinical practice. *Cartilage*. 2010;1(4):276-286.
19. Huang AH, Baker BM, Ateshian GA, Mauck RL. Sliding contact loading enhances the tensile properties of mesenchymal stem cell-seeded hydrogels. *Eur Cell Mater*. 2012;24:29-45.
20. Huang AH, Farrell MJ, Kim M, Mauck RL. Long-term dynamic loading improves the mechanical properties of chondrogenic mesenchymal stem cell-laden hydrogel. *Eur Cell Mater*. 2010;19:72-85.
21. Huang AH, Yeger-McKeever M, Stein A, Mauck RL. Tensile properties of engineered cartilage formed from chondrocyte- and MSC-laden hydrogels. *Osteoarthritis Cartilage*. 2008;16(9):1074-1082.
22. Ikenoue T, Trindade MC, Lee MS, et al. Mechanoregulation of human articular chondrocyte aggrecan and type II collagen expression by intermittent hydrostatic pressure in vitro. *J Orthop Res*. 2003;21(1):110-116.
23. Knutsen G, Engebretsen L, Ludvigsen TC, et al. Autologous chondrocyte implantation compared with microfracture in the knee: a randomized trial. *J Bone Joint Surg Am*. 2004;86(3):455-464.
24. Li WJ, Jiang YJ, Tuan RS. Cell-nanofiber-based cartilage tissue engineering using improved cell seeding, growth factor, and bioreactor technologies. *Tissue Eng Part A*. 2008;14(5):639-648.
25. Li Z, Yao SJ, Alini M, Stoddart MJ. Chondrogenesis of human bone marrow mesenchymal stem cells in fibrin-polyurethane composites is modulated by frequency and amplitude of dynamic compression and shear stress. *Tissue Eng Part A*. 2010;16(2):575-584.
26. Lin H, Cheng AW, Alexander PG, Beck AM, Tuan RS. Cartilage tissue engineering application of injectable gelatin hydrogel with in situ visible-light-activated gelation capability in both air and aqueous solution. *Tissue Eng Part A*. 2014;20(17-18):2402-2411.
27. Linsley CS, Wu BM, Tawil B. Mesenchymal stem cell growth on and mechanical properties of fibrin-based biomimetic bone scaffolds. *J Biomed Mater Res A*. 2016;104(12):2945-2953.
28. Lujan TJ, Wirtz KM, Bahney CS, Madey SM, Johnstone B, Bottlang M. A novel bioreactor for the dynamic stimulation and mechanical evaluation of multiple tissue-engineered constructs. *Tissue Eng Part C Methods*. 2011;17(3):367-374.
29. Marder RA, Hopkins G Jr, Timmerman LA. Arthroscopic microfracture of chondral defects of the knee: a comparison of two postoperative treatments. *Arthroscopy*. 2005;21(2):152-158.
30. Marsano A, Wendt D, Raiteri R, et al. Use of hydrodynamic forces to engineer cartilaginous tissues resembling the non-uniform structure and function of meniscus. *Biomaterials*. 2006;27(35):5927-5934.
31. Mauck RL, Byers BA, Yuan X, Tuan RS. Regulation of cartilaginous ECM gene transcription by chondrocytes and MSCs in 3D culture in response to dynamic loading. *Biomech Model Mechanobiol*. 2007;6(1-2):113-125.
32. Mayer-Wagner S, Hammerschmid F, Redeker JI, et al. Simulated microgravity affects chondrogenesis and hypertrophy of human mesenchymal stem cells. *Int Orthop*. 2014;38(12):2615-2621.
33. McAdams TR, Mithoefer K, Scopp JM, Mandelbaum BR. Articular cartilage injury in athletes. *Cartilage*. 2010;1(3):165-179.
34. McCormick F, Harris JD, Abrams GD, et al. Trends in the surgical treatment of articular cartilage lesions in the United States: an analysis of a large private-payer database over a period of 8 years. *Arthroscopy*. 2014;30(2):222-226.
35. Mithoefer K, Hambly K, Logerstedt D, Ricci M, Silvers H, Della Villa S. Current concepts for rehabilitation and return to sport after knee

articular cartilage repair in the athlete. *J Orthop Sports Phys Ther*. 2012;42(3):254-273.
36. Nugent-Derfus GE, Chan AH, Schumacher BL, Sah RL. PRG4 exchange between the articular cartilage surface and synovial fluid. *J Orthop Res*. 2007;25(10):1269-1276.
37. Nugent-Derfus GE, Takara T, O'Neill JK, et al. Continuous passive motion applied to whole joints stimulates chondrocyte biosynthesis of PRG4. *Osteoarthritis Cartilage*. 2007;15(5):566-574.
38. Pot MW, van Kuppevelt TH, Gonzales VK, et al. Augmented cartilage regeneration by implantation of cellular versus acellular implants after bone marrow stimulation: a systematic review and meta-analysis of animal studies. *PeerJ*. 2017;5:e3927.
39. Pound JC, Green DW, Roach HI, Mann S, Oreffo RO. An ex vivo model for chondrogenesis and osteogenesis. *Biomaterials*. 2007;28(18):2839-2849.
40. Remya NS, Nair PD. Mechanoresponsiveness of human umbilical cord mesenchymal stem cells in in vitro chondrogenesis—a comparative study with growth factor induction. *J Biomed Mater Res A*. 2016;104(10):2554-2566.
41. Richter DL, Schenck RC Jr, Wascher DC, Treme G. Knee articular cartilage repair and restoration techniques: a review of the literature. *Sports Health*. 2016;8(2):153-160.
42. Sakai S, Mishima H, Ishii T, et al. Rotating three-dimensional dynamic culture of adult human bone marrow-derived cells for tissue engineering of hyaline cartilage. *J Orthop Res*. 2009;27(4):517-521.
43. Salter RB. The biologic concept of continuous passive motion of synovial joints: the first 18 years of basic research and its clinical application. *Clin Orthop Relat Res*. 1989;242:12-25.
44. Schätti O, Grad S, Goldhahn J, et al. A combination of shear and dynamic compression leads to mechanically induced chondrogenesis of human mesenchymal stem cells. *Eur Cell Mater*. 2011;22:214-225.
45. Steadman JR, Rodkey WG, Rodrigo JJ. Microfracture: surgical technique and rehabilitation to treat chondral defects. *Clin Orthop Relat Res*. 2001;391(suppl):S362-S369.
46. Steinmetz NJ, Bryant SJ. The effects of intermittent dynamic loading on chondrogenic and osteogenic differentiation of human marrow stromal cells encapsulated in RGD-modified poly(ethylene glycol) hydrogels. *Acta Biomater*. 2011;7(11):3829-3840.
47. Taffetani M, Gottardi R, Gastaldi D, Raiteri R, Vena P. Poroelastic response of articular cartilage by nanoindentation creep tests at different characteristic lengths. *Med Eng Phys*. 2014;36(7):850-858.
48. Thorpe SD, Buckley CT, Vinardell T, O'Brien FJ, Campbell VA, Kelly DJ. Dynamic compression can inhibit chondrogenesis of mesenchymal stem cells. *Biochem Biophys Res Commun*. 2008;377(2):458-462.
49. Volz M, Schaumburger J, Frick H, Grifka J, Anders S. A randomized controlled trial demonstrating sustained benefit of autologous matrix-induced chondrogenesis over microfracture at five years. *Int Orthop*. 2017;41(4):797-804.
50. Waters RL, Lunsford BR, Perry J, Byrd R. Energy-speed relationship of walking: standard tables. *J Orthop Res*. 1988;6(2):215-222.
51. Williams JM, Moran M, Thonar EJ, Salter RB. Continuous passive motion stimulates repair of rabbit knee articular cartilage after matrix proteoglycan loss. *Clin Orthop Relat Res*. 1994;304:252-262.
52. Yoshioka T, Mishima H, Ohyabu Y, et al. Repair of large osteochondral defects with allogeneic cartilaginous aggregates formed from bone marrow-derived cells using RWV bioreactor. *J Orthop Res*. 2007;25(10):1291-1298.
53. Yu B, Yu D, Cao L, et al. Simulated microgravity using a rotary cell culture system promotes chondrogenesis of human adipose-derived mesenchymal stem cells via the p38 MAPK pathway. *Biochem Biophys Res Commun*. 2011;414(2):412-418.